

Modeling animal movement with directional persistence and attractive points

Gianluca Mastrantonio

Politecnico di Torino, Dipartimento di Scienze Matematiche

Abstract

GPS technology is more accessible to researchers and, nowadays, animal movement data are widely available. To analyze such data, different approaches have been proposed, and among them, hidden Markov models with the Ornstein-Uhlenbeck or the step-and-turn emission distribution are the most commonly used. The former characterizes movement with the use of a center of attraction, while the latter has directional persistence.

In this work we propose a new emission distribution that possesses the defining characteristics of the two aforementioned approaches, and at any given time, an animal can exhibit a different degree of directional persistence and attraction to a point in space.

Hidden Markov models based on our proposal, the Ornstein-Uhlenbeck, and the step-and-turn, are estimated on a real data example, where GPS locations of a Maremma Sheepdog are recorded. We show that our proposal has the richest output and better describes the data.

1 Introduction

The use of statistical models, to understand animal movement, has become increasingly popular. The data is generally in the form of a time series of 2-dimensional spatial locations recorded using a GPS device attached to the animal, with time-interval between observations programmed by the researcher (Cagnacci *et al.*, 2010). These data, often called "trajectory tracking data", allow investigating features of the animal movement, such as habitat selection (Hebblewhite and Merrill, 2008), spatiotemporal patterns (Morales *et al.*, 2004a; Fryxell *et al.*, 2008; Nathan *et al.*, 2008; Frair *et al.*, 2010) and animal behavior (Merrill and David Mech, 2000; Anderson and Lindzey, 2003); for a detailed review the reader may refer to Hooten *et al.* (2017). These approaches can be grouped into three main categories: point processes (Johnson *et al.*, 2013; Brost *et al.*, 2015), continuous-time dynamic models (CTM) (Blackwell, 1997; Johnson *et al.*, 2008; Fleming *et al.*, 2014) and discrete-time dynamic models (DTM) (Morales *et al.*, 2004a; Jonsen *et al.*, 2005; McClintock *et al.*, 2012).

In the CTM, the observed locations are seen as the finite-dimensional realization of a stochastic process, often the Ornstein-Uhlenbeck (OU) (Blackwell, 1997; Dunn and Gipson, 1977). In this approach, the animal is attracted to a specific spatial location, called *center of attraction*, which can be used to model a tendency toward a patch of space (McClintock *et al.*, 2012) or the home range (Christ *et al.*, 2008). In the DTM, the movement is described using the *movement-metrics*, i.e., the *step-length* and the *turning-angle* (ST), that are proxies of the speed and the direction between consecutive locations, observed at discrete time intervals; this approach allows to have directional persistence between consecutive steps (Jonsen *et al.*, 2005). Models based on the movement-metrics are often referred to as *step-and-turn* (ST) models.

Animal movement is a continuous process, and thus CTMs have a stronger theoretical justification, but from an interpretative point of view, it is easier to interpret and analyze movements using movement-metrics. On the other hand, movement-metrics have a coherent meaning only if the time-interval between observations is fixed (Codling and Hill, 2005; Patterson *et al.*, 2017). For a discussion

of the differences and similarities between the two models, the reader may refer to McClintock *et al.* (2014).

The need of capturing heterogeneity, which reflects changes in the behavior over time, has led to couple an *observational model*, either a DTM or CTM, with a *state model*, that describes the time evolution of the behavior (Patterson *et al.*, 2008). The introduction of switching between behavioral modes, which is generally assumed to be temporally structured, is limited in the context of CTM and in most cases is defined on a discrete-time scale (Hanks *et al.*, 2011; Kranstauber *et al.*, 2014), defeating the purpose of using a CTM; some exception exists (see for example Harris and Blackwell, 2013). On the other hand, DTM can be easily exploited in a state-space model, with discrete states in discrete time. In both approaches, conditionally to the state, the data are distributed accordingly to a parametric distribution, whose parameters depend on the latent state. In a DTM, independence between the movement-metrics is generally assumed, see for example Morales and Ellner (2002) or Patterson *et al.* (2017), and rarely they are dependent (Mastrantonio, 2018; Mastrantonio *et al.*, 2019). If the temporal switching between behaviors is assumed to follow a Markov process, as in many applications (see for example Michelot *et al.*, 2016; Langrock *et al.*, 2012), the model is said to be a hidden Markov model (HMM). In the HMM context, the observational model is also called emission distribution. This class of models is used due to the easiness of implementation and interpretation.

In this work we propose an HMM with a state-specific density that has as special cases the OU and the ST. To define our proposal, we envision the step-length and turning-angle as the polar coordinates representation of Cartesian coordinates. The latter is assumed to be normally distributed, which induces a normal distribution on the spatial locations. Since the distribution of the OU is also normal, we can combine the two by introducing a parameter $\rho \in [0, 1]$, defining a new normal distribution with mean and covariance matrix that reduces to the OU ones when $\rho = 0$ and the ST ones if $\rho = 1$. Then, the movement is biased toward the center of attraction and has a directional persistence for any value in between. Indeed, the closer is ρ to 0, and the stronger is the attraction and weaker the directional persistence, while the opposite is true, if it is close to 1. We call our proposal the *step-and-turn with an attractive point (STAP) model*. The STAP is used as emission distribution of the HMM, which allows us to detect, for any behavior, if it follows an OU dynamic, a ST dynamic, or a mixture of the two. Other proposals tried to combine the defining characteristics of the OU and ST, as McClintock *et al.* (2012) and Barton *et al.* (2009), but this is generally done using a ST model with direction mean that points to a spatial location, i.e., the attractive point.

To estimate the model, the number of latent behaviors is generally set a priori, see for example Langrock *et al.* (2012) or Morales *et al.* (2004b), and model selection is performed using informational criteria, e.g., the Integrated Classification Likelihood (ICL) (Biernacki *et al.*, 2000). Our HMM is formalized in a Bayesian framework, using the sticky hierarchical Dirichlet process HMM (sHDP-HMM) of Fox *et al.* (2011). The sHDP-HMM allows estimating, along with all the other model parameters, the number of latent behaviors, avoiding the use of informational criteria. The sHDP-HMM, with our proposal as emission distribution, is indicated as STAP-HMM.

We use our proposal to model the trajectory tracking data of a Maremma Sheepdog. For centuries, these dogs have been used in Europe and Asia to protect livestock from predators, and only recently in Australia (Gehring *et al.*, 2017; van Bommel and Johnson, 2016). They generally work with the shepherd in keeping the stock together, but, due to the properties extension, this is not always possible in Australia. Since the owner is often unaware of the dogs behavior, it is of interest to understand and characterize it. To study its behavior, we analyze a dataset, taken from the movebank repository (www.movebank.org), where the spatial locations of a dog, used to protect livestock in a property in Australia, are recorded using a GPS device (van and Johnson, 2014; van Bommel and Johnson, 2014). In this work we want to show that the model we propose is able to describe the behavior of this animal better than possible competitors and giving better insight into its movement patterns.

On the same dataset, sHDP-HMMs with OU (OU-HMM) and ST (ST-HMM) emission distributions are also estimated. We provide a comparison of the models results, highlighting differences and similarities, interpreting the behaviors found, the spatial distributions, and the hours of the day where the behaviors are more likely to be observed. We also show that our proposal produces a richer output,

showing that two of the five behaviors found follows a ST dynamic while the other 3 are OU.

The paper is organized as follows. In Section 2 we formalize the OU and ST models, that are used to build our proposal. In Section 3 the proposal is introduced as well as the sHDP-HMM while the real data application is in Section 4. The paper ends with some conclusive remarks, in Section 5.

2 The Ornstein-Uhlenbeck and the step-and-turn models

Let suppose to have a set of coordinates $\mathbf{s} = (\mathbf{s}_{t_1}, \mathbf{s}_{t_2}, \dots, \mathbf{s}_{t_T})'$, with $\mathbf{s}_t = (s_{t,1}, s_{t,2}) \in \mathcal{D} \subset \mathbb{R}^2$ and where t is a temporal index, assuming a fixed temporal distance between consecutive coordinates, i.e., they are regularly spaced in time.

2.1 The Ornstein-Uhlenbeck model

The time dynamic of a bivariate OU process can be written using the conditional density of the spatial location at time-point $t_i + \Delta t$ given the previously observed ones, where $\Delta t \in \mathbb{R}^+$, in the following way

$$\mathbf{s}_{t_i + \Delta t} | \mathbf{s}_{t_i} \sim N\left(\boldsymbol{\mu} + e^{\mathbf{B}\Delta t}(\mathbf{s}_{t_i} - \boldsymbol{\mu}), \boldsymbol{\Lambda} - e^{\mathbf{B}\Delta t} \boldsymbol{\Lambda} e^{\mathbf{B}'\Delta t}\right),$$

where \mathbf{B} is a 2×2 matrix and $\boldsymbol{\Lambda}$ is a covariance matrix (Dunn and Gipson, 1977). Notice that the process is first-order Markovian. Under the assumptions that $\lim_{\Delta t \rightarrow \infty} e^{\mathbf{B}\Delta t} = \mathbf{0}$, \mathbf{B} is said to be *stable*, and the long term distribution of the process is

$$\mathbf{s}_{t_i} \sim N(\boldsymbol{\mu}, \boldsymbol{\Lambda}).$$

If \mathbf{B} is stable, $\boldsymbol{\mu}$ can be interpreted as the central tendency and \mathbf{B} controls its form and strength. To simply inference, and also interpretation, matrix \mathbf{B} is often assumed to be isotropic, i.e. $\mathbf{B} = b\mathbf{I}_2$, with $b \leq 0$, as in Iglehart (1968). Under this assumption, the drift to the central coordinate $\boldsymbol{\mu}$ depends only on the spatial distance $\|\mathbf{s}_{t_i} - \boldsymbol{\mu}\|$; for a more discussion of the different parametrization of \mathbf{B} we refer the reader to Blackwell (1997).

Owing to the fixed time interval between observations, we can reparametrize the process in a way that is more suitable for our proposal:

$$\begin{aligned} \mathbf{s}_{t_{i+1}} &= \mathbf{s}_{t_i} + \nu(\boldsymbol{\mu} - \mathbf{s}_{t_i}) + \boldsymbol{\epsilon}_{t_i}, \\ \boldsymbol{\epsilon}_{t_i} &\sim N(\mathbf{0}, \boldsymbol{\Sigma}), \end{aligned} \tag{1}$$

where

$$\begin{aligned} \nu \mathbf{I} &= \mathbf{1} - e^{b\mathbf{I}_2(t_{i+1}-t_i)}, \\ \boldsymbol{\Sigma} &= \boldsymbol{\Lambda} - e^{b\mathbf{I}_2(t_{i+1}-t_i)} \boldsymbol{\Lambda} e^{b\mathbf{I}_2(t_{i+1}-t_i)}, \end{aligned} \tag{2}$$

or, equivalently

$$\mathbf{s}_{t_{i+1}} | \mathbf{s}_{t_i} \sim N(\mathbf{s}_{t_i} + \nu(\boldsymbol{\mu} - \mathbf{s}_{t_i}), \boldsymbol{\Sigma}). \tag{3}$$

From equation (2), we have $\nu \in [0, 1]$. When $\nu = 0$, the process is a two-dimensional random walk with no central drift, while $\nu = 1$ defines a model where the spatial locations are independent. The formulation given in (3) is the one that we are using in our proposal. Notice that it is easy to find the relation between ν and b , that is

$$b = \frac{\log(1 - \nu)}{t_{i+1} - t_i}.$$

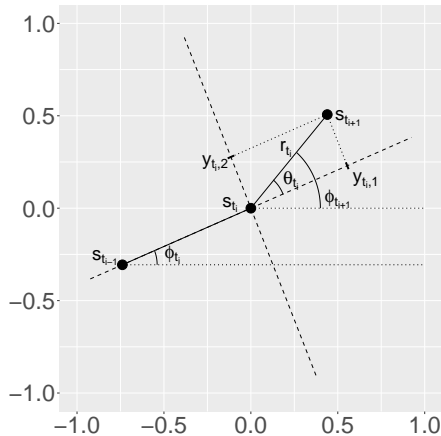


Figure 1: A graphical representation of the relation between the spatial locations, the movement-metrics and the displacement-coordinates.

2.2 The step-and-turn model

In the discrete-time framework, a probability distribution is generally defined for the movement-metrics instead of modeling directly the coordinates. Movement-metrics are a representation of the speed of the movement and an angle that measure how the animal turns. The most commonly used are the *step-length* $r_{t_i} = \|\mathbf{s}_{t_{i+1}} - \mathbf{s}_{t_i}\|_2 \in \mathbb{R}^+$, which is the distance traveled between two consecutive locations, and the *turning angle* $\theta_{t_i} \in [-\pi, \pi)$, which is the angle between $\mathbf{s}_{t_{i+1}}$ and \mathbf{s}_{t_i} onto the direction of the previous increment $\mathbf{s}_{t_i} - \mathbf{s}_{t_{i-1}}$, computed as $\theta_{t_i} = \phi_{t_{i+1}} - \phi_{t_i}$, where

$$\phi_{t_i} = \text{atan}^*(s_{t_i,2} - s_{t_{i-1},2}, s_{t_i,1} - s_{t_{i-1},1}), \quad (4)$$

and $\text{atan}^*(\cdot)$ is the two-argument tangent function (Jammalamadaka and Kozubowski, 2004). In Figure 1 we depict the relation between the spatial coordinates and the movement-metrics. With this approach is possible to model directional persistence, e.g, if the distribution of θ_{t_i} has small variance and circular mean equal to $-\pi/2$, between consecutive observations, the animal tends to turn to the right with an angle of $-\pi/2$.

In most applications, θ_{t_i} and r_{t_i} are assumed to be independent, see for example Parton and Blackwell (2017) or Morales *et al.* (2004a), but some exceptions exist (Mastrantonio, 2018; Mastrantonio *et al.*, 2019). Here, instead of modeling the movement-metrics directly, we see them as the polar coordinates representation of the Euclidian coordinates $\mathbf{y}_{t_i} = (y_{t_i,1}, y_{t_i,2})'$,

$$\begin{aligned} y_{t_i,1} &= r_{t_i} \cos(\theta_{t_i}), \\ y_{t_i,2} &= r_{t_i} \sin(\theta_{t_i}), \end{aligned}$$

called *displacement-coordinates*, see Figure 1, and we assume

$$\begin{aligned} \mathbf{y}_{t_i} &= \boldsymbol{\eta} + \boldsymbol{\epsilon}_{t_i}, \\ \boldsymbol{\epsilon}_{t_i} &\sim N(\mathbf{0}, \boldsymbol{\Sigma}), \end{aligned}$$

where $\boldsymbol{\eta} \in \mathbb{R}^2$ is a vector of length 2. Indeed, a distribution over \mathbf{y}_{t_i} induces a distribution for θ_{t_i} and r_{t_i} , which will be discussed in Section 3.

If we introduce the rotation matrix

$$\mathbf{R}(\omega) = \begin{pmatrix} \cos(\omega) & -\sin(\omega) \\ \sin(\omega) & \cos(\omega) \end{pmatrix}, \quad (5)$$

we have the following relations between the displacement-coordinates and the spatial locations:

$$\begin{aligned}\mathbf{y}_{t_i} &= \mathbf{R}(\phi_{t_i})' (\mathbf{s}_{t_{i+1}} - \mathbf{s}_{t_i}), \\ \mathbf{s}_{t_{i+1}} &= \mathbf{s}_{t_i} + \mathbf{R}(\phi_{t_i})\boldsymbol{\eta} + \mathbf{R}(\phi_{t_i})\boldsymbol{\epsilon}_{t_i}.\end{aligned}\tag{6}$$

Notice that, since ϕ_{t_i} is computed using \mathbf{s}_{t_i} and $\mathbf{s}_{t_{i-1}}$, see equation (4), the process is Markovian of the second order and

$$\mathbf{s}_{t_{i+1}}|\mathbf{s}_{t_i}, \mathbf{s}_{t_{i-1}} \sim N(\mathbf{s}_{t_i} + \mathbf{R}(\phi_{t_i})\boldsymbol{\eta}, \mathbf{R}(\phi_{t_i})\boldsymbol{\Sigma}\mathbf{R}(\phi_{t_i})').\tag{7}$$

3 The step-and-turn with an attractive point and the hidden Markov model

The OU and ST models have different features, useful in the description of animal movement, that are, respectively, the attractive point and the directional persistence. Our idea is to combine the two to have a model that possess both features with different degree, e.g., the movement can be highly biased toward an attractive point with a moderate directional persistence.

As we can see from equations (1) and (7), due to the distributional assumption on \mathbf{y} , both approaches model the conditional distribution of $\mathbf{s}_{t_{i+1}}$ as a normal. We combine the two in a more general model, assuming

$$\mathbf{s}_{t_{i+1}}|\mathbf{s}_{t_i}, \mathbf{s}_{t_{i-1}} \sim N(\mathbf{M}_{t_i}, \mathbf{V}_{t_i}),$$

where we allow $(\mathbf{M}_{t_i}, \mathbf{V}_{t_i})$ to have the values of equation (1) and (7). We first focus on parameter \mathbf{V}_{t_i} , which is the variance of the conditional distribution, that is equal to $\boldsymbol{\Sigma}$ and $\mathbf{R}(\phi_{t_i})\boldsymbol{\Sigma}\mathbf{R}(\phi_{t_i})'$ for, respectively, the OU and the ST. If the rotation matrix argument is 0, we have $\mathbf{R}(0) = \mathbf{I}$ (see equation (5)) and $\mathbf{R}(\phi_{t_i})\boldsymbol{\Sigma}\mathbf{R}(\phi_{t_i})'$ reduces to $\boldsymbol{\Sigma}$. We then introduce the parameter $\rho \in [0, 1]$, which multiplies ϕ_{t_i} and changes the argument of $\mathbf{R}(\cdot)$. The covariance matrix \mathbf{V}_{t_i} is then defined as

$$\mathbf{V}_{t_i} = \mathbf{R}(\rho\phi_{t_i})\boldsymbol{\Sigma}\mathbf{R}(\rho\phi_{t_i})'.\tag{8}$$

For the mean vector we follow a similar approach. Here, again, we want to have a parameter that allows us to move from the mean of the OU to the one of the ST, respectively equal to $\mathbf{s}_{t_i} + \nu(\boldsymbol{\mu} - \mathbf{s}_{t_i})$ and $\mathbf{s}_{t_i} + \mathbf{R}(\phi_{t_i})\boldsymbol{\eta}$. We use the same parameter ρ of equation (8), and define

$$\mathbf{M}_{t_i} = \mathbf{s}_{t_i} + (1 - \rho)\nu(\boldsymbol{\mu} - \mathbf{s}_{t_i}) + \rho\mathbf{R}(\rho\phi_{t_i})\boldsymbol{\eta}.$$

The conditional distribution of our proposal, that we call step-and-turn with an attractive point, is then

$$\mathbf{s}_{t_{i+1}}|\mathbf{s}_{t_i}, \mathbf{s}_{t_{i-1}} \sim N(\mathbf{s}_{t_i} + (1 - \rho)\nu(\boldsymbol{\mu} - \mathbf{s}_{t_i}) + \rho\mathbf{R}(\rho\phi_{t_i})\boldsymbol{\eta}, \mathbf{R}(\rho\phi_{t_i})\boldsymbol{\Sigma}\mathbf{R}(\rho\phi_{t_i})').\tag{9}$$

If $\rho = 0$, equation (9) is equal to (3), while (9) reduces to (7) if $\rho = 1$. For $\rho \in (0, 1)$, the animal is attracted to the spatial point $\boldsymbol{\mu}$, as in the OU model, but, since through the rotation matrix $\mathbf{R}(\rho\phi_{t_i})$ the movement is affected by the previous direction, it shows also some degree of directional persistence, as in the ST model. Notice that our proposal adds only a single parameter to be able to model OU and ST behaviors.

The displacement-coordinates of our model can be computed as

$$\mathbf{R}(\phi_{t_i})'(1 - \rho)\nu(\boldsymbol{\mu} - \mathbf{s}_{t_i}) + \rho\mathbf{R}(\phi_{t_i})'\mathbf{R}(\rho\phi_{t_i})\boldsymbol{\eta} + \mathbf{R}(\phi_{t_i})'\mathbf{R}(\rho\phi_{t_i})\boldsymbol{\epsilon}_{t_i},$$

see equation (6), and they are normally distributed.

It is well known that the angle of the polar coordinates of a bivariate normal random variable, i.e., θ_{t_i} , is projected normal distributed (Wang and Gelfand, 2013), which is one of the most flexible distributions for circular data, see for example Mastrantonio *et al.* (2016) or Maruotti *et al.* (2016). The projected normal can be very helpful since is the only circular distribution that can be bimodal. On the other hand, the distribution of the step-length can be computed in closed-form only in special cases, e.g., if $\boldsymbol{\Sigma}$ is diagonal, then r_{t_i} has a Rice distribution (Kobayashi *et al.*, 2011), while if the mean is 0, the step-length is Hoyt distributed (Hoyt, 1947).

STAP-HMM	OU-HMM	ST-HMM
-7523283.903	-7760842.59	-7689036.136

Table 1: ICL index of the estimated models. The best value is in bold.

3.1 The hidden Markov model

In equation (9), parameters do not change with time. This hypothesis is unrealistic, since it is reasonable to assume that an animal exhibits different behaviors over time, which results in different movement characteristics and likelihood parameters. To introduce heterogeneity, it is generally assumed that the data come from a mixture-type model. Different approaches have been proposed, see for example Patterson *et al.* (2017), Harris and Blackwell (2013) or Mastrantonio *et al.* (2019), but the most commonly used is the HMM. Under this model, the behavior is coded by a discrete random variable $z_{t_i} \in Z \subseteq \mathbb{N}$ whose value indicates the behavior that the animal is following at time t_i , and the temporal evolution is generated by a first-order Markov process. We decide to define the HMM under the non-parametric Bayesian framework, using the the sHDP-HMM (Fox *et al.*, 2011). Then, let

$$\mathbf{M}_{t_i,j} = \mathbf{s}_{t_i} + (1 - \rho_j)\nu_j (\boldsymbol{\mu}_j - \mathbf{s}_{t_i}) + \rho_j \mathbf{R}(\rho_j \phi_{t_i}) \boldsymbol{\eta}_j$$

and

$$\mathbf{V}_{t_i,j} = \mathbf{R}(\rho_j \phi_{t_i}) \boldsymbol{\Sigma}_j \mathbf{R}(\rho_j \phi_{t_i})',$$

the proposed model is:

$$\begin{aligned} \mathbf{s}_{t_{i+1}} | \mathbf{s}_{t_i}, \mathbf{s}_{t_{i-1}}, \mathbf{M}_{t_i, \mathbf{s}_{t_i}}, \mathbf{V}_{t_i, \mathbf{s}_{t_i}} &\sim N(\mathbf{M}_{t_i, \mathbf{s}_{t_i}}, \mathbf{V}_{t_i, \mathbf{s}_{t_i}}), \quad i = 1, \dots, T-1, \\ \mathbf{s}_{t_0} &\sim \text{Unif}(\mathcal{D}), \\ z_{t_i} | z_{t_{i-1}}, \boldsymbol{\pi}_{z_{t_i}} &\sim \text{Multinomial}(1, \boldsymbol{\pi}_{z_{t_{i-1}}}), \quad i = 1, \dots, T-1, \\ z_{t_0} &= 1, \\ \boldsymbol{\pi}_j | \alpha, \kappa, \boldsymbol{\beta} &\sim \text{Dir}\left(\alpha + \kappa, \frac{\alpha \boldsymbol{\beta} + \kappa \delta_j}{\alpha + \kappa}\right), \quad j \in \mathbb{N}, \\ \boldsymbol{\beta} | \gamma &\sim \text{GEM}(\gamma), \\ \boldsymbol{\xi}_j &\sim H, \quad j \in \mathbb{N}, \end{aligned} \tag{10}$$

where $\boldsymbol{\pi}_j$ and $\boldsymbol{\beta}$ are infinite-dimensional probability vectors, $\boldsymbol{\xi}_j = (\rho_j, \nu_j, \boldsymbol{\mu}_j, \boldsymbol{\eta}_j, \boldsymbol{\Sigma}_j)$, $\text{GEM}(\cdot)$ indicate the Griffiths-Engen-McCloskey distribution (Ishwaran and Zarepour, 2002), and δ_j is the Dirac-delta. To define the conditional distribution of the observations we need \mathbf{s}_{t_0} , that here is assumed to come from a uniform distribution over the observed domain \mathcal{D} . Notice that in (10) the number of possible behaviors is infinite, since $\boldsymbol{\pi}_j$ is infinite-dimensional but in the observed time-window only a finite number of them can be observed. The K unique values assumed by $\{z_{t_i}\}_{i=1}^{T-1}$ is a random variable that can be used to estimate the number of latent behaviors.

4 Real data

Maremma Sheepdogs are dogs of large breeds, originated from Italy, used for centuries all over Europe and Asia to protect livestock from predators and thieves. These dogs, from an early age, are trained to live with the livestock, creating a strong bond and then adult dogs view the livestock as their social companions, protecting them from threats for the rest of their life. Recent studies proved that Sheepdogs are effective in protecting livestock from a wide range of potential predators (Gehring *et al.*, 2017; van Bommel and Johnson, 2016). The dogs can be fence-trained, to remain in proximity of the paddock where the livestock are confined, but they are generally allowed to cross fences, move freely, and roam over large areas.

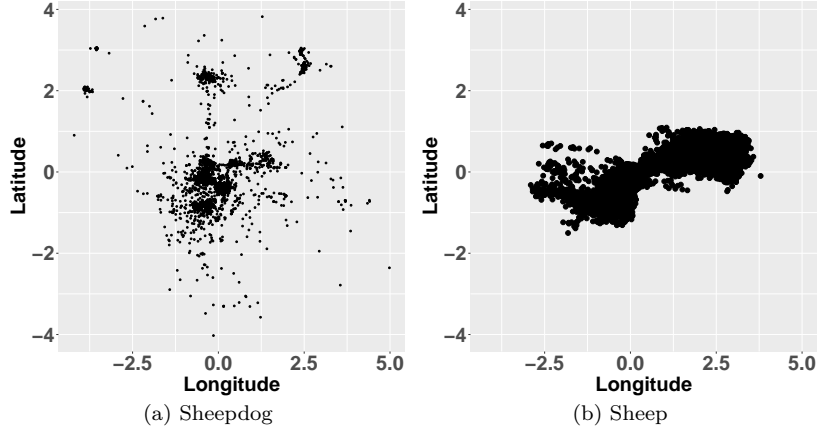


Figure 2: Spatial locations of the Maremma Sheepdog (a) and sheep (b).

	j=1	j=2	j=3	j=4	j=5
$\hat{\mu}_{j,1}$	0.559	0.804	18.024	-0.443	0.179
(CI)	(-64.41 62.873)	(-60.404 61.796)	(-13.302 62.592)	(-2.153 -0.281)	(0.169 0.189)
$\hat{\mu}_{j,2}$	-0.338	0.251	6.235	-0.322	-0.404
(CI)	(-62.685 63.304)	(-62.459 62.19)	(-21.542 41.287)	(-0.685 -0.21)	(-0.413 -0.395)
$\hat{\eta}_{j,1}$	-0.005	-0.043	-0.389	2.093	-0.555
(CI)	(-0.006 -0.004)	(-0.057 -0.028)	(-62.227 60.293)	(-60.5 63.858)	(-64.229 58.681)
$\hat{\eta}_{j,2}$	0	-0.001	0.363	0.53	-0.31
(CI)	(-0.001 0.001)	(-0.013 0.01)	(-62.21 64.219)	(-58.338 60.591)	(-60.833 60.093)
$\hat{\nu}_j$	0.502	0.501	0.007	0.625	0.985
(CI)	(0.025 0.973)	(0.024 0.978)	(0 0.036)	(0.573 0.677)	(0.973 0.997)
$\hat{\rho}_j$	1	1	0	0.002	0
(CI)	(1 1)	(1 1)	[0 0]	[0 0.023]	[0 0]
$\hat{\Sigma}_{j,1,1}$	0.001	0.029	0.801	0.127	0.006
(CI)	(0.001 0.001)	(0.022 0.039)	(0.681 0.955)	(0.102 0.156)	(0.005 0.008)
$\hat{\Sigma}_{j,1,2}$	0	0	-0.076	0.032	0.001
(CI)	(0 0)	(-0.002 0.002)	(-0.137 -0.021)	(0.017 0.048)	(0 0.001)
$\hat{\Sigma}_{j,2,2}$	0.001	0.017	0.404	0.159	0.005
(CI)	(0.001 0.001)	(0.014 0.023)	(0.341 0.485)	(0.132 0.19)	(0.004 0.006)
$\hat{\pi}_{j,1}$	0.848	0.073	0.024	0.044	0.011
(CI)	(0.834 0.86)	(0.062 0.084)	(0.017 0.032)	(0.035 0.054)	(0.005 0.019)
$\hat{\pi}_{j,2}$	0.287	0.386	0.151	0.092	0.085
(CI)	(0.241 0.338)	(0.333 0.437)	(0.114 0.19)	(0.056 0.131)	(0.057 0.114)
$\hat{\pi}_{j,3}$	0.068	0.197	0.517	0.162	0.055
(CI)	(0.038 0.106)	(0.14 0.261)	(0.447 0.585)	(0.112 0.216)	(0.026 0.089)
$\hat{\pi}_{j,4}$	0.17	0.21	0.001	0.41	0.209
(CI)	(0.124 0.221)	(0.149 0.277)	(0 0.008)	(0.332 0.484)	(0.165 0.256)
$\hat{\pi}_{j,5}$	0.876	0	0.006	0.002	0.115
(CI)	(0.775 0.978)	(0 0.003)	(0 0.033)	(0 0.026)	(0.019 0.213)

Table 2: Posterior means and CIs of the STAP-HMM parameters, under K=5.

In Australia, and outside the country of origin, the use of Maremma Sheepdogs (or general livestock guardian dogs) is relatively new and the interest in their use is increasing (van Bommel and Invasive Animals Cooperative Research Centre, 2010). Owing to the properties extension, which can be several thousand hectares in area, is hard, or even impossible, for the owner to supervision the dogs (van Bommel and Johnson, 2012), which are visited rarely, sometimes only once a week. The owner is, therefore, unaware of the dog movements and behavior (van Bommel and Invasive Animals Cooperative Research Centre, 2010).

In this section, using data taken from the movebank repository (www.movebank.org), which contains datasets, freely available, of GPS coordinates of a wide range of animals, we want to model and understand the behavior of a Maremma Sheepdog in Australia. The dataset¹ contains GPS locations of Maremma Sheepdogs and sheep on three properties (van and Johnson, 2014). The dataset has been

¹available at the address <https://www.datarepository.movebank.org/handle/10255/move.395>

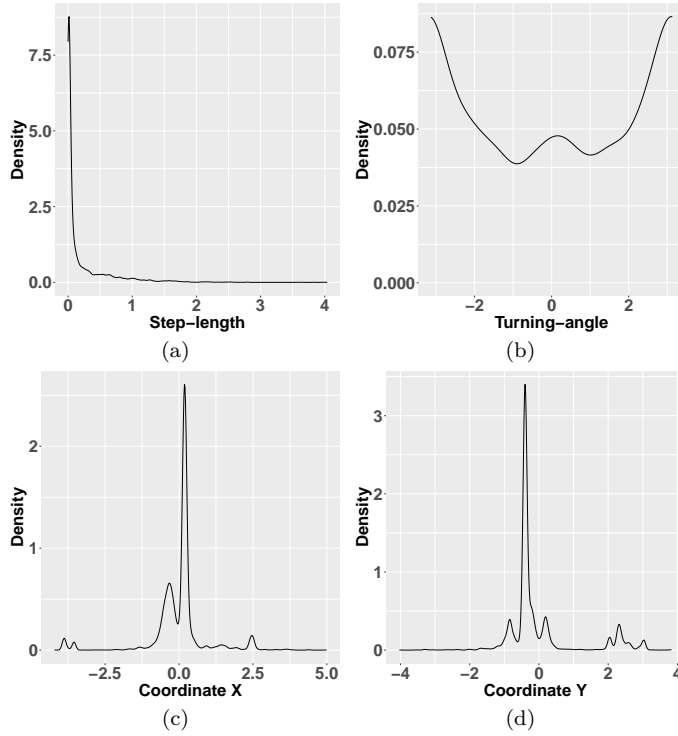


Figure 3: Distributions of the observed movement-metrics ((a) and (b)) and coordinates ((c) and (d)).

	j=1	j=2	j=3	j=4	j=5
$\hat{\mu}_{j,1}$	-3.168	-0.105	17.062	-0.356	0.18
(CI)	(-52.457 43.823)	(-22.525 23.693)	(-15.255 59.094)	(-0.423 -0.295)	(0.17 0.19)
$\hat{\mu}_{j,2}$	-0.294	3.153	5.021	-0.314	-0.404
(CI)	(-46.638 45.392)	(-7.564 31.502)	(-25.564 41.621)	(-0.389 -0.244)	(-0.412 -0.395)
$\hat{\nu}_j$	0	0.008	0.008	0.624	0.985
(CI)	(0 0)	(0 0.02)	(0 0.038)	(0.572 0.681)	(0.974 0.996)
$\hat{\Sigma}_{j,1,1}$	0.001	0.035	0.854	0.12	0.006
(CI)	(0.001 0.001)	(0.025 0.05)	(0.709 1.062)	(0.097 0.15)	(0.005 0.007)
$\hat{\Sigma}_{j,1,2}$	0	-0.002	-0.083	0.031	0.001
(CI)	(0 0)	(-0.005 0.001)	(-0.155 -0.023)	(0.015 0.047)	(0 0.002)
$\hat{\Sigma}_{j,2,2}$	0.001	0.019	0.427	0.164	0.005
(CI)	(0.001 0.001)	(0.014 0.027)	(0.357 0.522)	(0.134 0.204)	(0.004 0.006)
$\hat{\pi}_{j,1}$	0.847	0.077	0.023	0.042	0.011
(CI)	(0.834 0.86)	(0.066 0.089)	(0.015 0.031)	(0.032 0.052)	(0.005 0.019)
$\hat{\pi}_{j,2}$	0.28	0.396	0.143	0.085	0.096
(CI)	(0.236 0.33)	(0.338 0.458)	(0.102 0.185)	(0.048 0.125)	(0.067 0.126)
$\hat{\pi}_{j,3}$	0.07	0.209	0.504	0.161	0.056
(CI)	(0.039 0.107)	(0.148 0.276)	(0.429 0.571)	(0.11 0.217)	(0.026 0.093)
$\hat{\pi}_{j,4}$	0.17	0.19	0	0.447	0.193
(CI)	(0.125 0.22)	(0.123 0.262)	(0 0.006)	(0.359 0.526)	(0.151 0.24)
$\hat{\pi}_{j,5}$	0.883	0	0.004	0.003	0.11
(CI)	(0.777 0.979)	(0 0.003)	(0 0.029)	(0 0.026)	(0.017 0.212)

Table 3: Posterior means and CIs of the OU-HMM parameters, under K=5.

previously analyzed by van Bommel and Johnson (2014), and the authors, using tests and descriptive statistics, estimated home-ranges, activity patterns and path tortuosity.

Among the available data, we select a subset of temporally-contiguous observations of one dog, called “Bindi”, which belongs to the “Rivesdale” property, situated in North-East Victoria. Its locations are recorded every 30 minutes, starting from 2010-03-13 at 18:30, to 2010-07-23 at 17:33. The data, that consist of 6335 time-points with 196 missings, are plotted in Figure 2 (a); notice that, to facilitate

	j=1	j=2	j=3
$\hat{\eta}_{j,1}$	-0.005	-0.044	0.026
(CI)	(-0.006 -0.004)	(-0.059 -0.029)	(-0.021 0.073)
$\hat{\eta}_{j,2}$	0	0.001	-0.008
(CI)	(-0.001 0.001)	(-0.009 0.011)	(-0.046 0.029)
$\hat{\Sigma}_{j,1,1}$	0.001	0.036	0.597
(CI)	(0.001 0.001)	(0.029 0.045)	(0.541 0.657)
$\hat{\Sigma}_{j,1,2}$	0	0	0.013
(CI)	(0 0)	(-0.002 0.002)	(-0.017 0.042)
$\hat{\Sigma}_{j,2,2}$	0.001	0.018	0.394
(CI)	(0.001 0.001)	(0.015 0.022)	(0.357 0.435)
$\hat{\pi}_{j,1}$	0.849	0.086	0.064
(CI)	(0.837 0.861)	(0.074 0.099)	(0.055 0.075)
$\hat{\pi}_{j,2}$	0.349	0.415	0.236
(CI)	(0.308 0.394)	(0.364 0.463)	(0.198 0.274)
$\hat{\pi}_{j,3}$	0.245	0.213	0.543
(CI)	(0.213 0.279)	(0.168 0.256)	(0.501 0.583)

Table 4: Posterior means and CIs of the ST-HMM parameters, under K=3.

the priors specification, the coordinates are centered and divided by a pooled variance. The observed sheep coordinates are shown in Figure 2 (b).

In Figure 3, we depicted the kernel density estimates of the observed movement-metrics and coordinates. Both OU and ST models can be fitted to the data since a clear bimodality can be seen in the turning-angle distribution, which suggests a ST-HMM, as well as different modes on the coordinates, that can be attractive points.

4.1 Computational details

We estimate our proposal (STAP-HMM) and the competitive models OU-HMM and ST-HMM. For all models, we use weakly informative priors for the likelihood parameters, namely $N(\mathbf{0}_1, 1000\mathbf{I}_2)$ for $\boldsymbol{\mu}_j$ and $\boldsymbol{\eta}_j$, $\boldsymbol{\Sigma}_j \sim IW(3, \mathbf{I})$, a uniform over $[0, 1]$ for ϕ_j . For parameter ρ_j we define a prior that is a mixture of a uniform over $(0, 1)$, with weight equal to $1/3$, and two probability masses, one over 0 and one over 1, with probability $1/3$ each. This prior allows posterior samples of ρ_j to assume the value 0 and 1 with probability greater than 0.

We also assume (α, κ, γ) , i.e., the parameters of the latent classification, to be random variables. Following Fox *et al.* (2011), closed-form expression for the update of these parameters can be achieved if we define $\lambda_1 = \alpha + \kappa$ and $\lambda_2 = \kappa/(\alpha + \kappa)$ with the following priors: $\lambda_1 \sim G(a_1, b_1)$, $\lambda_2 \sim B(a_2, b_2)$, and $\gamma \sim G(a_\gamma, b_\gamma)$, where $B(\cdot, \cdot)$ stands for the beta distribution and $G(\cdot, \cdot)$ for the gamma. The priors are $\lambda_1 \sim G(0.1, 1)$, $\lambda_2 \sim B(10, 1)$, $\gamma \sim G(0.1, 1)$. These priors are used to avoid the production of redundant behaviors, i.e., behaviors with similar vector of likelihood parameters, that is a known problem of the DP-based models (Fox *et al.*, 2011) by assuming a prior over K , evaluated through simulations, that is almost fully concentrated on 1. This means that we are assuming (a-priori) that only one behavior is observed, i.e., the model is not a mixture, and if the data strongly support the hypothesis of different behaviors, the posterior of K will move away from the prior.

The model is estimated using an MCMC algorithm with 50000 iterations, burnin 30000, thin 4. The MCMC implementation is straightforward since, with the exception of the likelihood parameters, we can use the work of Fox *et al.* (2011) to obtain posterior samples. On the other hand, owing to the normal (conditional) distribution of the observed locations, the full conditional of $\boldsymbol{\mu}_j$, $\boldsymbol{\eta}_j$, and $\boldsymbol{\Sigma}_j$ can be obtained in closed-form using standard results, while ν_j and ρ_j are updated with Metropolis steps. For all models, convergence was established using the *coda* package (Plummer *et al.*, 2006) of R. The models are implemented in Julia 1.3 (Bezanson *et al.*, 2017) and the code to replicate the results are available at https://github.com/GianlucaMastrantonio/STAP_HMM_model.

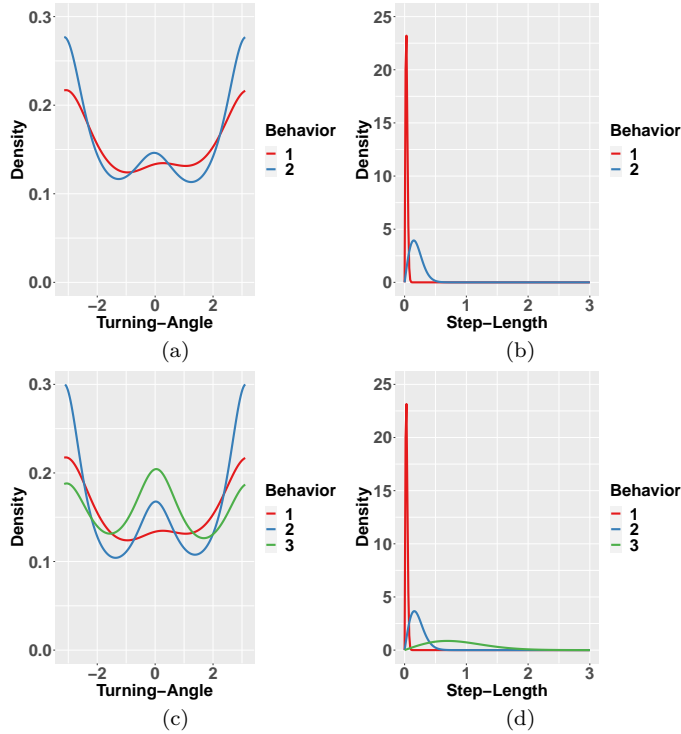


Figure 4: Turning-angle (first column) and step-length (second column) distributions for the first two behaviors of the STAP-HMM (first row) and all behaviors of the ST-HMM (second row).

4.2 The results

We compare the models performance with the ICL (Biernacki *et al.*, 2000) and in Table 1 the results are shown. The index suggests that our model fits the data better. As suggested by Pohle *et al.* (2017), we think that is also important to compare models from an interpretative point of view to see which one gives a better insight on the animal movement. Then, we first describe the results obtained with our proposal, and then we compare the models.

For each model and time-point, we compute the maximum at posterior estimate of z_{t_i} , indicated with \hat{z}_{t_i} , and we call it the *MAP behaviors*. The number of unique values of \hat{z}_{t_i} is the estimate of the number of behaviors K . For both STAP-HMM and OU-HMM, K is equal to 5 (behaviors), while $K = 3$ for the ST-HMM. The posterior means (indicated using the hat notation $\hat{\cdot}$) and CIs of all model parameters are shown in Tables 2, 3 and 4. To simplify the discussion, we indicate with LB_j the j -th latent behavior under our model, while $LB_{j,OU}$ and $LB_{j,ST}$ are the ones under the OU-HMM and ST-HMM, respectively.

STAP-HMM results Parameter ρ , in both LB_1 and LB_2 , has CI $(1,1]$, suggesting that they are ST states. The posterior densities of turning-angles and step-lengths for the ST part of these behaviors, i.e. $\mathbf{R}(\phi_{t_i})\boldsymbol{\eta}_1 + \mathbf{R}(\phi_{t_i})\boldsymbol{\epsilon}_{t_i}$, are depicted in Figure 4 (a) and (b), showing that LB_1 has slower speed, with respect to LB_2 , and both have a bimodal circular distribution with major mode at around $-\pi$ and a smaller one at 0. These modes indicate that the dog tends to move on the opposite direction of the previous movement (mode at $-\pi$) or on the same direction (mode at 0); the latter is less likely.

In Figure 5, for each behavior is shown the proportion of time that the associate value of \hat{z}_{t_i} is observed at a given time-point. We can see that LB_1 is more probable during the central hours and less during the night. On the other hand, LB_2 has larger values during the night. From Figure 6 (a) and (b), we see that LB_1 and LB_2 share, approximatively, the same spatial locations. We don't have

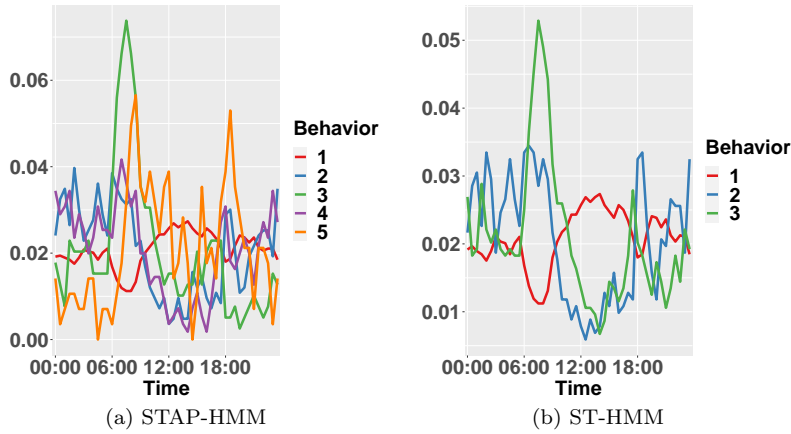


Figure 5: For each behavior, the line represents the proportion of times (y-axis) that is selected at a given hour (x-axis).

the coordinates of the property boundaries, but they can be seen in van Bommel and Johnson (2014), Figure 1, second row, and it is clear that LB_1 and LB_2 are inside the property boundaries.

These two behaviors represent the boundary patrolling or scent-marking, which is a common behavior of Maremma Sheepdog (Black and Green, 1985; I and M.E., 1999), where the higher speed of the second, is mostly related to the predator incursions (van Bommel and Johnson, 2014), which is more likely during the night. The behavior LB_1 , owing to the very low speed, can also represent the resting behavior.

LB_3 is an OU-type behavior (the CI of ρ_j is $[0, 0)$), characterized by the absence of an attractive point, since $\hat{\nu}$ is almost 0, and the CIs of $\mu_{3,1}$ and $\mu_{3,2}$ contain the entire spatial domain. It is more probable to observe it in the first hours of the morning, and the animal goes outside the property boundaries, as we can see from Figure 6 (c). This can be interpreted as exploratory behavior.

The fourth behavior, LB_4 , is an OU-type ($\rho \approx 0$), with spatial locations mostly overlapping with the ones of the sheep (Figure 6 (d)), and an attractive point ($\hat{\mu}_4$) located in the area where the livestock paddock is, see Figure 2 (b). The parameter ν_4 has posterior mean equal to 0.625, which shows a moderate attraction to $\hat{\mu}_4$, and it is more likely during the night. This is the behavior that represents the dog attending livestock at the core of the property.

The last behavior is again an OU-type ($\hat{\rho}_5 = 0$) with a strong attraction to μ_5 ($\hat{\nu}_5 = 0.985$). The spatial locations are similar to the one of LB_4 and the behavior is more likely during the central hours of the day, with two spikes in the first hours of the morning and before sunset. Differently from all the others, where $\hat{\pi}_{jj} > \hat{\pi}_{jj'}$ for $j \neq j'$, here $\hat{\pi}_{55} < \hat{\pi}_{51'} = 0.876$. The paper of van Bommel and Johnson (2014) (Figure 1, second row) shows that there is a self-feeder, where the dog can obtain dry food ad-lib, approximatively located at the spatial location $\hat{\mu}_5$, i.e., the attractive point of LB_5 . This can be interpreted as the feeding behavior and, after feeding, the dog switches to a boundary patrolling/resting behavior, which is represented by LB_1 .

OU-HMM results We can easily compare the MAP behaviors under the STAP- and OU-HMM, showing the proportion of time that the j -th behavior of the STAP-HMM is observed at the same temporal indices of the l -th behavior of the OU-HMM. The results are depicted in Figure 7 (a). From the figure is clear that the animal behaviors under the two models have the same temporal dynamic, i.e., the animal exhibits behavior LB_j and $LB_{j,OU}$ at the same temporal points. This almost one-to-one relation explains why the parameter estimates of LB_3 , LB_4 and LB_5 , i.e. the OU-type behaviors of our proposal, are very similar to $LB_{3,OU}$, $LB_{4,OU}$ and $LB_{5,OU}$, respectively (see Tables 2 and 3).

Having the same temporal evolution of the STAP-HMM, the behaviors have the same spatial locations and time of the day where they are more likely to be observed. This means that the interpretation

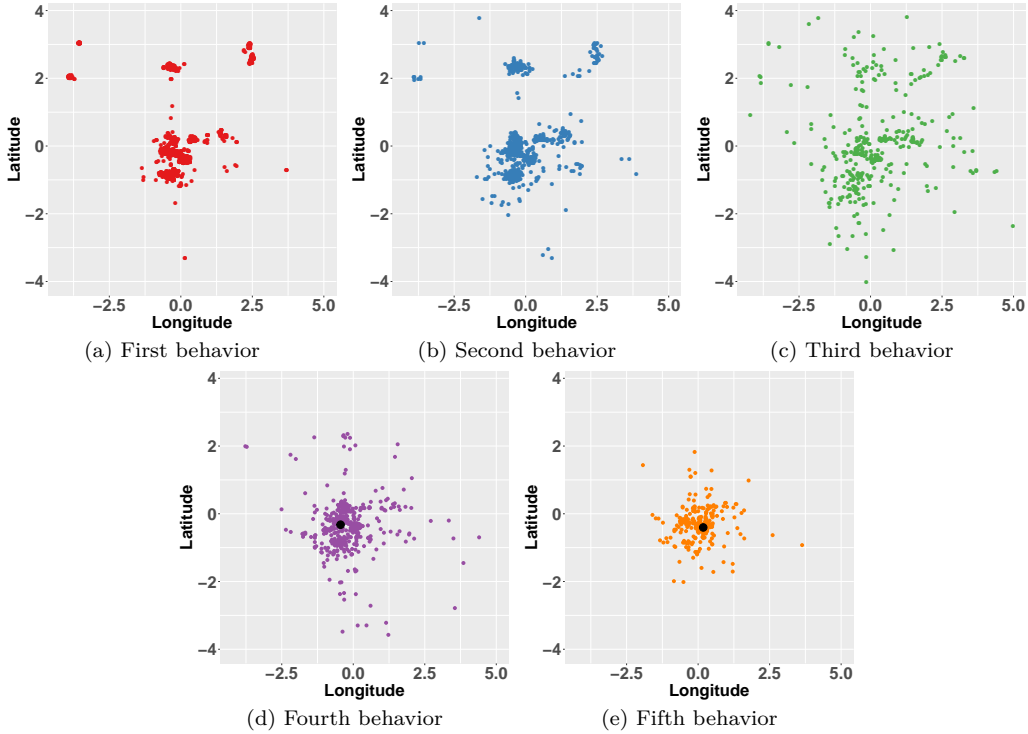


Figure 6: Spatial locations of the MAP behavior under the STAP-HMM model. In (d) and (e) the black dot represents $\hat{\mu}_4$ and $\hat{\mu}_5$, respectively.

is similar, but, on the other hand, the OU-HMM fails to recognize the directional persistence that are present in the first and second behavior, and estimates a random walk with no attractive point, i.e., $\hat{\nu}_1 = 0$ and $\hat{\nu}_2 = 0.008$, respectively.

We want to demonstrate that the OU-HMM is not appropriate to describe data on the first and second behavior. Even though the OU is not formalized in terms of the movement-metrics, it induce a distribution over the step-length and turning-angle, and they are not known in closed-form. We can simulate animal paths, with parameters given by the posterior mean values of the first and second OU-HMM behaviors, and then estimate the distribution of the movement-metrics. In Figure 8 we show the kernel density estimate of the observed turning-angle distributions, computed using only data with temporal indices that belong to the first two OU-HMM MAP behaviors, i.e., $z_{t_i} = 1$ or $z_{t_i} = 2$, while in Figure 9 the turning-angle distributions are computed using the simulated paths, which are composed of 50000 time-points. As we can see the turning-angles of Figure 8 closely resemble the ones estimated by the STAP-HMM, while in the OU-HMM case the turning-angles are almost uniformly distributed.

ST-HMM results The ST-HMM estimate only 3 behaviors, and the posterior densities of the movement-metrics are shown in Figure 4 (c) and (d). As we can see from Figure 7 (b), the dog follows LB_1 and $LB_{1,ST}$ at the same temporal points, which is also shown by the spatial location of $LB_{1,ST}$, that can be seen in Figure 10 (a). Posterior estimates of the likelihood parameters are almost identical, and this can be also verified by the posterior densities in Figure 4 (c) and (d).

$LB_{2,ST}$ has mostly the same temporal indices of LB_2 , similar spatial locations (Figure 10 (b)), frequencies during the day (Figure 5 (b)), step-length distribution (Figure 4 (d)), but a different circular one (Figure 4 (c)). With respect to $LB_{1,ST}$, this behavior has a higher speed, a bimodal circular distribution with the major mode at $-\pi$ and a smaller one at 0. As LB_2 , this behavior can be interpreted as boundary patrolling or protection from predator incursions.

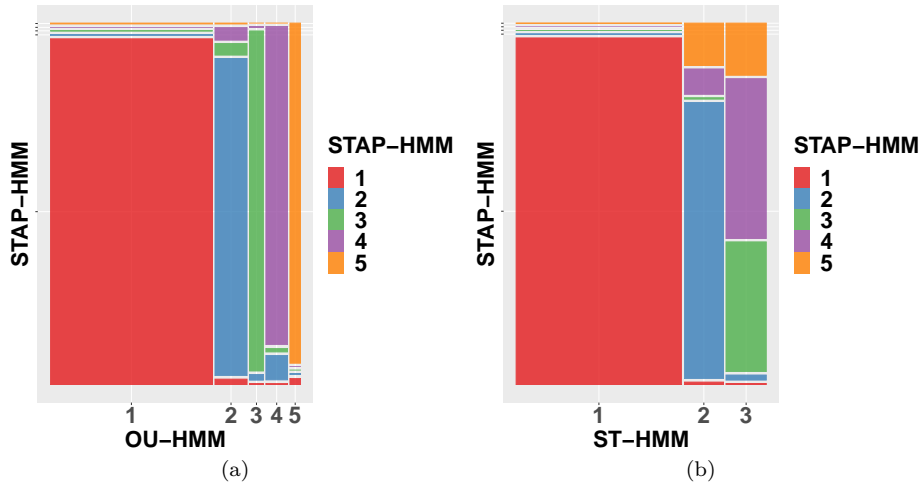


Figure 7: Graphical representation of the two-way table between MAP behaviors under different models: (a) STAP-HMM and OU-HMM; (b) STAP-HMM and ST-HMM. The area is proportional to the frequency.

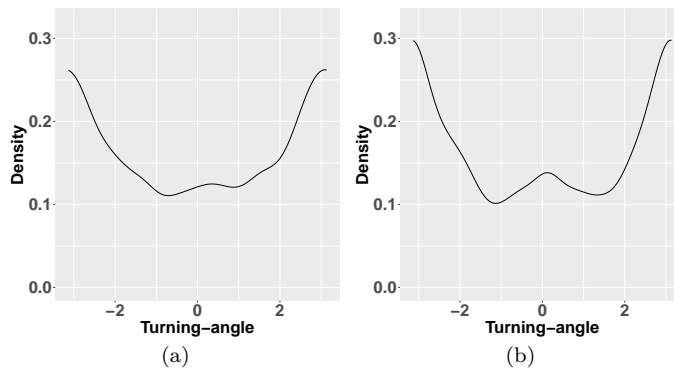


Figure 8: Observed turning-angle distributions computed using the data that belong to the temporal indices of the first (a) and second (b) OU-HMM MAP behaviors.

The last behavior, $LB_{3,ST}$, has the highest speed and circular distribution with two modes, approximately with the same density, at 0 and $-\pi$, see Figure 4 (c) and (d). It is more likely during the night or the first hours of the morning. Since the spatial distribution is similar to the one of LB_3 , we can interpret this behavior as the exploring one.

General comments Our proposal is able to estimate behaviors that are similar, in interpretation and posterior inference, to $LB_{3,OU}$, $LB_{4,OU}$, $LB_{5,OU}$ and $LB_{1,ST}$, as well as to find a behavior, LB_2 , that is not estimated by the others two. The ST-HMM finds three behaviors but, since none of them has spatial distribution concentrated on the livestock paddock, as the $LB_{4,STAP}$ and $LB_{5,STAP}$, it does not identify the dog attending livestock. The OU-HMM fails to find structure in $LB_{1,OU}$ and $LB_{2,OU}$, where it estimates a simple random walk, while we shows (see Figures 8 and 9) that there is directional persistence.

From an interpretative point of view, our model is able to find 5 behaviors. The first one, owing to the low speed, is the resting behavior and, as the second one, the dog remains inside the boundaries (see Figure 6 (a) and (b)). The second one has higher speed, as can be seen in Figure 4 (b), and since it is more likely during the night, see Figure 5 (a), is the behavior where the dog is protecting livestock

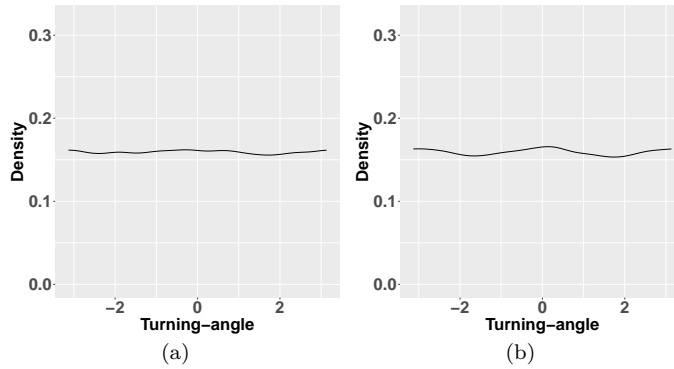


Figure 9: Turning-angle distributions of the first (a) and second (b) OU-HMM MAP behaviors.

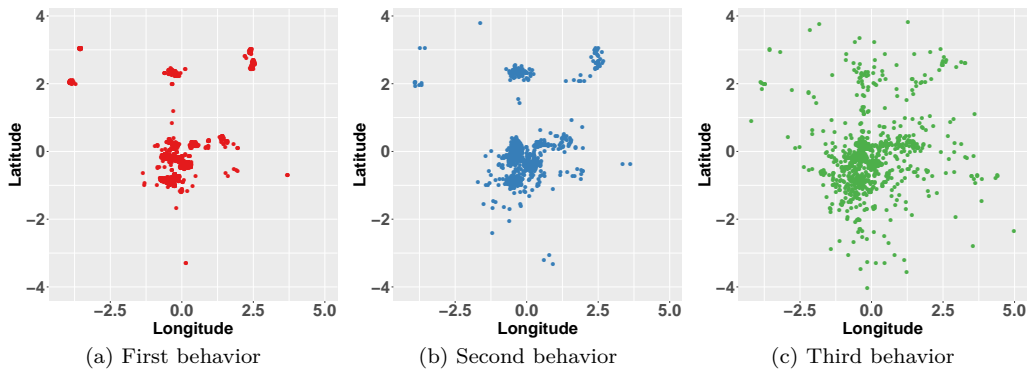


Figure 10: Spatial locations of the MAP behavior under the ST-HMM model.

from predator incursions. In the third one the dog is exploring, since it goes outside the property boundaries, and it is the behavior that has most of the spatial locations far away from the livestock. As already pointed out by van Bommel and Invasive Animals Cooperative Research Centre (2010), Maremma Sheepdogs tend to leave the livestock in the first morning hours, and this is confirmed by Figure 5 (a). In the last two, the dog remains in the proximity of the livestock, with differences in the time of the day where they are more likely: $LB_{4,STAP}$ during the night, $LB_{5,STAP}$ during the day. When the dog is in $LB_{5,STAP}$, there is a high probability that in the following time-point, the behavior will switch to the resting one, i.e., $LB_{1,STAP}$ (see row $\hat{\pi}_{j,5}$ in Table 2).

The results clearly show that our proposal has a richer output, better ICL, and is able to identify the different types of movements that the animal exhibits, indicating clearly when this is based on an OU or a ST model. For this reason, we believe that our proposal is the one that better describes the data.

5 Final remarks

In this work we introduced a new model that can be used to analyze animal movement data. Our proposal can be seen as a generalization of the two state-of-the-art models used, generally, in this context, namely the OU and the ST. In our proposal the animal can be attracted to a spatial point, as in the OU, but showing directional persistence, as in the ST, at the same time. We were able to do this by introducing only a further parameter, other than the ones related to the ST and OU approaches.

The proposed models, the OU-HMM, and ST-HMM, were estimated on a real data example, where the spatial locations of a Maremma Sheepdog are recorded. We compared the results of the

three approaches, showing differences and similarities. While all of them gave a good description of the animal movement, our proposal was the one with the richest output, better interpretation and goodness-of-fit.

Before this proposal, we tried to combine the ST and OU approaches using a likelihood defined as a mixture of the two but, although it seemed promising, it worked only when used without the HMM. When multiple behaviors were assumed, identifiability problems arose between the mixtures in the data likelihood and the mixture defines by the HMM. In the future, we will investigate further this type of model to see if the identification problems can be solved. Moreover, we will extend our model to incorporate multiple animals, as in Langrock *et al.* (2014), and we will use more flexible temporal dynamics for the latent behavior switching, as in Harris and Blackwell (2013) or Mastrantonio *et al.* (2019).

Acknowledgement

This work has partially been developed under the MIUR grant Dipartimenti di Eccellenza 2018 - 2022 (E11G18000350001), conferred to the Dipartimento di Scienze Matematiche - DISMA, Politecnico di Torino.

References

- Anderson, C. R. and Lindzey, F. G. (2003). Estimating cougar predation rates from gps location clusters. *The Journal of Wildlife Management*, **67**(2), 307–316.
- Barton, K. A., Phillips, B. L., Morales, J. M., and Travis, J. M. J. (2009). The evolution of an ‘intelligent’ dispersal strategy: biased, correlated random walks in patchy landscapes. *Oikos*, **118**(2), 309–319.
- Bezanson, J., Edelman, A., Karpinski, S., and Shah, V. B. (2017). Julia: A fresh approach to numerical computing. *SIAM review*, **59**(1), 65–98.
- Biernacki, C., Celeux, G., and Govaert, G. (2000). Assessing a mixture model for clustering with the integrated completed likelihood. *IEEE Trans. Pattern Anal. Mach. Intell.*, **22**(7), 719–725.
- Black, H. and Green, J. (1985). Navajo use of mixed-breed dogs for management of predators. *Journal of Range Management*, **38**(1), 11–15.
- Blackwell, P. (1997). Random diffusion models for animal movement. *Ecological Modelling*, **100**(1), 87 – 102.
- Brost, B. M., Hooten, M. B., Hanks, E. M., and Small, R. J. (2015). Animal movement constraints improve resource selection inference in the presence of telemetry error. *Ecology*, **96**(10), 2590–2597.
- Cagnacci, F., Boitani, L., Powell, R. A., and Boyce, M. S. (2010). Animal ecology meets gps-based radiotelemetry: a perfect storm of opportunities and challenges. *Philosophical Transactions of the Royal Society of London B: Biological Sciences*, **365**(1550), 2157–2162.
- Christ, A., Hoef, J. V., and Zimmerman, D. L. (2008). An animal movement model incorporating home range and habitat selection. *Environmental and Ecological Statistics*, **15**(1), 27–38.
- Codling, E. and Hill, N. (2005). Sampling rate effects on measurements of correlated and biased random walks. *Journal of Theoretical Biology*, **233**(4), 573 – 588.
- Dunn, J. E. and Gipson, P. S. (1977). Analysis of radiotelemetry data in studies of home range. *Biometrics*, **33**(1).

- Fleming, C. H., Calabrese, J. M., Mueller, T., Olson, K. A., Leimgruber, P., and Fagan, W. F. (2014). Non-markovian maximum likelihood estimation of autocorrelated movement processes. *Methods in Ecology and Evolution*, **5**(5), 462–472.
- Fox, E. B., Sudderth, E. B., Jordan, M. I., and Willsky, A. S. (2011). A sticky hdp-hmm with application to speaker diarization. *The Annals of Applied Statistics*, **5**(2A), 1020–1056.
- Frair, J. L., Fieberg, J., Hebblewhite, M., Cagnacci, F., DeCesare, N. J., and Pedrotti, L. (2010). Resolving issues of imprecise and habitat-biased locations in ecological analyses using gps telemetry data. *Philosophical Transactions of the Royal Society of London B: Biological Sciences*, **365**(1550), 2187–2200.
- Fryxell, J. M., Hazell, M., Börger, L., Dalziel, B. D., Haydon, D. T., Morales, J. M., McIntosh, T., and Rosatte, R. C. (2008). Multiple movement modes by large herbivores at multiple spatiotemporal scales. *Proceedings of the National Academy of Sciences*, **105**(49), 19114–19119.
- Gehring, T. M., VerCauteren, K. C., and Cellar, A. C. (2017). Good fences make good neighbors: Implementation of electric fencing for establishing effective livestock-protection dogs. *Human-Wildlife Interactions*, **5**(1), 106–111.
- Hanks, E. M., Hooten, M. B., Johnson, D. S., and Sterling, J. T. (2011). Velocity-based movement modeling for individual and population level inference. *PLOS ONE*, **6**(8), 1–17.
- Harris, K. J. and Blackwell, P. G. (2013). Flexible continuous-time modelling for heterogeneous animal movement. *Ecological Modelling*, **255**, 29 – 37.
- Hebblewhite, M. and Merrill, E. (2008). Modelling wildlife and human relationships for social species with mixed-effects resource selection models. *Journal of Applied Ecology*, **45**(3), 834–844.
- Hooten, M., Johnson, D., McClintock, B., and Morales, J. (2017). *Animal Movement: Statistical Models for Telemetry Data*. CRC Press.
- Hoyt, R. S. (1947). Probability functions for the modulus and angle of the normal complex variate. *Bell System Technical Journal*, **26**(2), 318–359.
- I, H. and M.E., S. (1999). Livestock-guarding dogs in norway part ii: Different working regimes. *Journal of Range Management*, **52**(1), 312–316.
- Iglehart, D. L. (1968). Limit theorems for the multi-urn ehrenfest model. *Ann. Math. Statist.*, **39**(3), 864–876.
- Ishwaran, H. and Zarepour, M. (2002). Exact and approximate sum representations for the Dirichlet process. *Canadian Journal of Statistics*, **30**(2), 269–283.
- Jammalamadaka, S. R. and Kozubowski, T. J. (2004). New families of wrapped distributions for modeling skew circular data. *Communications in Statistics - Theory and Methods*, **33**(9), 2059–2074.
- Johnson, D. S., London, J. M., Lea, M.-A., and Durban, J. W. (2008). Continuous-time correlated random walk model for animal telemetry data. *Ecology*, **89**(5), 1208–1215.
- Johnson, D. S., Hooten, M. B., and Kuhn, C. E. (2013). Estimating animal resource selection from telemetry data using point process models. *Journal of Animal Ecology*, **82**(6), 1155–1164.
- Jonsen, I. D., Flemming, J. M., and Myers, R. A. (2005). Robust state-space modeling of animal movement data. *Ecology*, **86**(11), 2874–2880.

- Kobayashi, H., Mark, B. L., and Turin, W. (2011). *Probability, Random Processes, and Statistical Analysis: Applications to Communications, Signal Processing, Queueing Theory and Mathematical Finance*. Cambridge University Press.
- Kranstauber, B., Safi, K., and Bartumeus, F. (2014). Bivariate gaussian bridges: directional factorization of diffusion in brownian bridge models. *Movement Ecology*, **2**(1), 5.
- Langrock, R., King, R., Matthiopoulos, J., Thomas, L., Fortin, D., and Morales, J. M. (2012). Flexible and practical modeling of animal telemetry data: hidden Markov models and extensions. *Ecology*, **93**(11), 2336–2342.
- Langrock, R., Hopcraft, G., Blackwell, P., Goodall, V., King, R., Niu, M., Patterson, T., Pedersen, M., Skarin, A., and Schick, R. (2014). Modelling group dynamic animal movement. *Methods in Ecology and Evolution*, **5**(2), 190–199.
- Maruotti, A., Punzo, A., Mastrantonio, G., and Lagona., F. (2016). A time-dependent extension of the projected normal regression model for longitudinal circular data based on a hidden Markov heterogeneity structure. *Stochastic Environmental Research and Risk Assessment*, **30**, 1725–1740.
- Mastrantonio, G. (2018). The joint projected normal and skew-normal: A distribution for polycylindrical data. *Journal of Multivariate Analysis*, **165**, 14 – 26.
- Mastrantonio, G., Jona Lasinio, G., and Gelfand, A. E. (2016). Spatio-temporal circular models with non-separable covariance structure. *TEST*, **23**, 331–350.
- Mastrantonio, G., Grazian, C., Mancinelli, S., and Bibbona, E. (2019). New formulation of the logistic-gaussian process to analyze trajectory tracking data. *Ann. Appl. Stat.*, **13**(4), 2483–2508.
- McClintock, B. T., King, R., Thomas, L., Matthiopoulos, J., McConnell, B. J., and Morales, J. M. (2012). A general discrete-time modeling framework for animal movement using multistate random walks. *Ecological Monographs*, **82**(3), 335–349.
- McClintock, B. T., Johnson, D. S., Hooten, M. B., Ver Hoef, J. M., and Morales, J. M. (2014). When to be discrete: the importance of time formulation in understanding animal movement. *Movement Ecology*, **2**(1), 21.
- Merrill, S. B. and David Mech, L. (2000). Details of extensive movements by minnesota wolves (*canis lupus*). *The American Midland Naturalist*, **144**(2), 428–433.
- Michelot, T., Langrock, R., and Patterson, T. A. (2016). movehmm: an r package for the statistical modelling of animal movement data using hidden markov models. *Methods in Ecology and Evolution*, **7**(11), 1308–1315.
- Morales, J. M. and Ellner, S. P. (2002). Scaling up animal movements in heterogeneous landscapes: the importance of behavior. *Ecology*, **83**(8), 2240–2247.
- Morales, J. M., Haydon, D. T., Frair, J., Holsinger, K. E., and Fryxell, J. M. (2004a). Extracting more out of relocation data: building movement models as mixtures of random walks. *Ecology*, **85**(9), 2436–2445.
- Morales, J. M., Haydon, D. T., Frair, J., Holsinger, K. E., and Fryxell, J. M. (2004b). Extracting more out of relocation data: building movement models as mixtures of random walks. *Ecology*, **85**(9), 2436–2445.
- Nathan, R., Getz, W. M., Revilla, E., Holyoak, M., Kadmon, R., Saltz, D., and Smouse, P. E. (2008). A movement ecology paradigm for unifying organismal movement research. *Proceedings of the National Academy of Sciences*, **105**(49), 19052–19059.

- Parton, A. and Blackwell, P. G. (2017). Bayesian inference for multistate ‘step and turn’ animal movement in continuous time. *Journal of Agricultural, Biological and Environmental Statistics*, **22**(3), 373–392.
- Patterson, T., Thomas, L., Wilcox, C., Ovaskainen, O., and Matthiopoulos, J. (2008). State-space models of individual animal movement. *Trends in Ecology & Evolution*, **23**(2), 87–94.
- Patterson, T. A., Parton, A., Langrock, R., Blackwell, P. G., Thomas, L., and King, R. (2017). Statistical modelling of individual animal movement: an overview of key methods and a discussion of practical challenges. *AStA Advances in Statistical Analysis*, **101**(4), 399–438.
- Plummer, M., Best, N., Cowles, K., and Vines, K. (2006). Coda: Convergence diagnosis and output analysis for mcmc. *R News*, **6**(1), 7–11.
- Pohle, J., Langrock, R., van Beest, F. M., and Schmidt, N. M. (2017). Selecting the number of states in hidden markov models: Pragmatic solutions illustrated using animal movement. *Journal of Agricultural, Biological and Environmental Statistics*, **22**(3), 270–293.
- van Bommel, L. and Johnson, C. (2014). Data from: Where do livestock guardian dogs go? movement patterns of free-ranging maremme sheepdogs, doi:10.5441/001/1.pv048q7v.
- van Bommel, L. and Invasive Animals Cooperative Research Centre (2010). *Guardian Dogs: Best Practice Manual for the Use of Livestock Guardian Dogs*. Invasive Animals Cooperative Research Centre.
- van Bommel, L. and Johnson, C. N. (2012). Good dog! using livestock guardian dogs to protect livestock from predators in australia’s extensive grazing systems. *Wildlife Research*, **39**(3), 220–229.
- van Bommel, L. and Johnson, C. N. (2014). Where do livestock guardian dogs go? movement patterns of free-ranging maremme sheepdogs. *PLOS ONE*, **9**(10), 1–12.
- van Bommel, L. and Johnson, C. N. (2016). Livestock guardian dogs as surrogate top predators? how maremme sheepdogs affect a wildlife community. *Ecology and Evolution*, **6**(18), 6702–6711.
- Wang, F. and Gelfand, A. E. (2013). Directional data analysis under the general projected normal distribution. *Statistical Methodology*, **10**(1), 113–127.